New Journal of Physics
The open access journal at the forefront of physics

Deutsche Physikalische Gesellschaft DPG
IOP Institute of Physics

Published in partnership with: Deutsche Physikalische Gesellschaft and the Institute of Physics

OPEN ACCESS

RECEIVED
18 July 2016

REVISED
23 August 2016

ACCEPTED FOR PUBLICATION
2 September 2016

PUBLISHED
27 September 2016

PAPER

Effects of scalar leptoquark on semileptonic Λ_b decays

Suchismita Sahoo and Rukmani Mohanta[1]

School of Physics, University of Hyderabad, Hyderabad -500046, India
[1] Author to whom any correspondence should be addressed.

E-mail: rmsp@uohyd.ernet.in

Keywords: semileptonic Λ_b decays, leptoquark model, LFV decays

Abstract

We study the scalar leptoquark effects on the rare semileptonic decays of Λ_b baryon, governed by the quark level transition $b \to s l^+ l^-$. We estimate the branching ratios, forward–backward asymmetries, lepton polarisation parameters and the lepton flavour non-universality effects in these decay channels. We find significant deviations from the corresponding standard model predictions in some of the observables due to leptoquark effects. We also investigate the lepton flavour violating decays $\Lambda_b \to \Lambda l_i^- l_j^+$, the branching ratios of which are found to be $\mathcal{O}(10^{-10} - 10^{-9})$.

1. Introduction

The study of the rare B meson decays involving flavour changing neutral current (FCNC) transitions is very crucial, as they provide sensitive probe to look for new physics (NP) beyond the standard model (SM). These decays are highly suppressed in the SM due to Glashow–Iliopoulos–Maiani mechanism and occur only through one-loop level penguin and box diagrams. Recently, several anomalies have been observed in the rare semileptonic B decays mediated through the FCNC $b \to s$ transitions. The most prominent ones are the observation of 3.7σ deviation in the angular observable P_5' [1–3] of $B \to K^* \mu^+ \mu^-$ mode and the violation of lepton universality in the $B \to K l^+ l^-$ decays at the level of 2.6σ [4] by the LHCb experiment. In addition, LHCb has also observed significant discrepancy in the decay rates of the $B \to K^* l^+ l^-$ processes [5, 6]. Also the decay rate of the $B_s \to \phi \mu^+ \mu^-$ process [7] has 3.3σ deviation form its SM value in the low q^2 region. Furthermore, the observed discrepancy in the ratio of branching fractions of exclusive $B \to K^{(*)} l^+ l^-$ decay and the inclusive decays into dimuon over dielectron in the full q^2 range [8] provide strong evidence of the presence of lepton non-universality.

The anomalies observed in $b \to s l^+ l^-$ processes at LHCb [1, 2, 4–7] have attracted a lot of attention in recent times. The implications of these observations have been extensively studied both in the context of various NP models and in model independent ways [9–13]. These deviations which are at the level of $(2–3)\sigma$ are not statistically significant enough to provide an unambiguous signal of NP. On the other hand they are also not small enough to be ignored completely and need to be scrutinized meticulously as many different ways as possible. If indeed they really evince the smoking gun signal of some kind of NP, such effects must also show up in other decay channels involving $b \to s$ transitions, such as the corresponding Λ_b transitions. Therefore, the study of the rare Λ_b decays is of utmost importance to obtain an unambiguous signal of NP. Including the baryonic decay mode $\Lambda_b \to \Lambda(\to p\pi^-)\mu^+\mu^-$ in the Bayesian analysis of $|\Delta B| = |\Delta S| = 1$ transitions, a fit of the Wilson coefficients $C_{9,10}$, $C'_{9,10}$ has been performed in [14], and it has been shown that, the shift to C_9 prefers to be opposite to the one found in mesonic case. To be more specific, the shift in C_9 in baryonic decay is found to be $\Delta_9 = C_9 - C_9^{\rm SM} = 1.6^{+0.7}_{-0.9}$, as compared to the mesonic case where its value is $\Delta_9 = -1.09^{+0.22}_{-0.20}$ [11]. Whereas the corresponding shifts in C_{10} are in the same direction, i.e., $\Delta_{10} = 0.7^{+0.5}_{-0.8}$ for the baryonic case $\Delta_{10} = 0.56^{+0.25}_{-0.24}$ for mesonic case. As pointed out in [14], the observed discrepancy in the shift of C_9 might arise from our incomplete understanding of the hadronic matrix elements of the two-point correlators of $\mathcal{O}_{1,\cdots,6;8}$ with the quark electromagnetic current, which effectively shift the Wilson coefficients C_7 and C_9. This could also be due to the large experimental uncertainties for the $\Lambda_b \to \Lambda(\to p\pi)\mu^+\mu^-$ observables. However, if this

persists with improved statistics, this would constitute a breakdown of the universal structure of the transversity amplitudes at low recoil, as predicted by the operator product expansion.

The important distinction between the Λ_b baryon and B meson decays is the spin of the Λ_b baryon. Therefore, the number of degrees of freedom involved in the bound state of baryon is more, hence the systematic study of $\Lambda_b \to \Lambda\gamma$ and $\Lambda_b \to \Lambda\mu^+\mu^-$ are relatively less explored in comparison to their mesonic counter parts. Also the experimental data on various Λ_b decay channels are rather limited. Recently LHCb has reported the branching ratio of $\Lambda_b \to \Lambda\mu^+\mu^-$ [15], which is found to be lower than its SM prediction. This decay process has been extensively studied in the literature both in the SM and in various beyond the SM scenarios [16–23]. To supplement these studies, in this paper we would like to analyze the rare baryonic decay processes $\Lambda_b \to \Lambda l^+l^-$, where $l = e,\ \mu,\ \tau$ in the scalar leptoquark model. In recent times, the scalar leptoquark model has been received a lot of attention, as it can successfully explain most of the observed anomalies associated with the $b \to sll$ transitions. Leptoquarks are colour-triplet bosonic particles which can couple to a quark and lepton pair at the same time. The existence of leptoquark has been proposed in many extensions of the SM, such as grand unification model [24, 25], Pati–Salam model [26], extended technicolour model [27] and the composite models [28]. The leptoquark states can be classified as vectors (spin-1) or scalars (spin-0). They can be characterised by their Fermion no. $F = 3B + L$, where B and L are the baryon no. and lepton no. respectively. Scalar leptoquarks may exist at TeV scale, and can give observable signatures in various low energy processes [33]. The phenomenology of scalar leptoquarks has been studied extensively in the literature [29–37]. In this paper, we would like to study the rare baryonic decay processes $\Lambda_b \to \Lambda l^+l^-$ in the scalar leptoquark model. In particular, we estimate the decay rates, forward–backward ($A_{\rm FB}$) and lepton polarisation asymmetries in these modes. Furthermore, we explore the possibility of lepton non-universality parameter in Λ_b decays and also the lepton flavour violating (LFV) decays mediated via the scalar leptoquarks.

The paper is organised as follows. In section 2 we present the effective Hamiltonian responsible for the $b \to sl^+l^-$ processes and the decay parameters for the semileptonic $\Lambda_b \to \Lambda l^+l^-$ decays in the SM. The NP contribution due to the exchange of scalar leptoquark has been presented in section 3 and the constraints on the leptoquark parameter space has been obtained by using the measured branching ratios of the rare decays $B_s \to l^+l^-$. In section 4, we present the numerical analysis for the branching ratios and other physical observables such as the forward–backward asymmetry, lepton polarisation asymmetry and the lepton non-universality by using the constrained leptoquark couplings. We compute the branching ratios of the LFV $\Lambda_b \to \Lambda l_i^- l_j^+$ decays in sections 5 and 6 contains the summary and conclusion.

2. Theoretical framework for the analysis of $\Lambda_b \to \Lambda l^+l^-$ decay process

In this section, we will discuss the SM contributions to the branching ratios and other physical observables of the $\Lambda_b \to \Lambda l^+l^-, l = e,\ \mu,\ \tau$ processes. The effective Hamiltonian describing the decay process $\Lambda_b \to \Lambda l^+l^-$ involves the quark level transition $b \to sl^+l^-$ and is given by [38]

$$\mathcal{H}_{\rm eff} = -\frac{4G_{\rm F}}{\sqrt{2}} V_{tb}V_{ts}^* \Bigg[\sum_{i=1}^{6} C_i(\mu)O_i + C_7\frac{e}{16\pi^2}(\bar{s}\sigma_{\mu\nu}(m_sP_L + m_bP_R)b)\mathrm{F}^{\mu\nu} + C_9^{\rm eff}\frac{\alpha}{4\pi}(\bar{s}\gamma^\mu P_L b)\bar{l}\gamma_\mu l + C_{10}\frac{\alpha}{4\pi}(\bar{s}\gamma^\mu P_L b)\bar{l}\gamma_\mu\gamma_5 l\Bigg], \quad (1)$$

where $V_{qq'}$ are the CKM matrix elements, $G_{\rm F}$ denotes the Fermi constant, α is the fine-structure constant, C_i's are the Wilson coefficients evaluated at the renormalized scale $\mu = m_b$ [39] and $P_L,\ P_R = (1 \mp \gamma_5)/2$ are the chiral operators. The sum over i includes the current–current operators $i = 1,\ 2$ and the QCD-penguin operators $i = 3,\ 4,\ 5,\ 6$.

In addition to the short distance contributions these processes also receive additional contributions arising from the long distance effects due to the real $c\bar{c}$ resonant states of $J/\psi,\ \psi'$, i.e., $\Lambda_b \to \Lambda J/\psi(\psi') \to \Lambda l^+l^-$. These resonance contributions can be included by modifying the Wilson coefficient C_9. Thus, the modified coefficient ($C_9^{\rm eff}$) contains a perturbative part and a resonance part which can be written as

$$C_9^{\rm eff} = C_9^{\rm SM} + Y(s) + C_9^{\rm res}, \quad (2)$$

where $C_9^{\rm SM}$ is the SM Wilson coefficient evaluated at the b quark mass scale [39], the perturbative part $Y(s)$ receives contributions coming from one-loop matrix elements of the four quark operators [40] and the long distance resonance effect is given by [41]

$$C_9^{\rm res} = \frac{3\pi}{\alpha^2}(3C_1 + C_2 + 3C_3 + C_4 + 3C_5 + C_6)\sum_{V_i=\psi(1S),\cdots,\psi(6S)} \kappa_{V_i}\frac{m_{V_i}\Gamma(V_i \to l^+l^-)}{m_{V_i}^2 - s - {\rm i}m_{V_i}\Gamma_{V_i}}. \quad (3)$$

Here the phenomenological parameter κ is taken to be 1.65 and 2.36 [42] for the lowest resonances J/ψ and ψ' respectively in order to reproduce the correct branching ratio of $\mathcal{B}(B \to J/\psi K^* \to K^* l^+ l^-) = \mathcal{B}(B \to J/\psi K^*)\mathcal{B}(J/\psi \to l^+ l^-)$.

The matrix elements of the hadronic currents in (1) between initial Λ_b and the final Λ baryon can be parameterised in terms of various form factors which are presented in appendix A. Thus, using these matrix elements, the transition amplitude for the $\Lambda_b \to \Lambda l^+ l^-$ processes can be written as [16, 18]

$$\begin{aligned}\mathcal{M}(\Lambda_b \to \Lambda l^+ l^-) = \frac{G_F\,\alpha}{\sqrt{2}\,\pi} V_{tb} V_{ts}^* [\bar{l}\gamma_\mu l\{\bar{u}_\Lambda(\gamma^\mu(A_1 P_R + B_1 P_L) + \mathrm{i}\sigma^{\mu\nu} q_\nu (A_2 P_R + B_2 P_L))u_{\Lambda_b}\} \\ + \bar{l}\gamma_\mu\gamma_5 l\{\bar{u}_\Lambda(\gamma^\mu(D_1 P_R + E_1 P_L) + \mathrm{i}\sigma^{\mu\nu} q_\nu (D_2 P_R + E_2 P_L) \\ + q^\mu (D_3 P_R + E_3 P_L))u_{\Lambda_b}\}],\end{aligned} \tag{4}$$

where the parameters A_i, B_i, D_j and E_j with $i = 1, 2$, $j = 1, 2, 3$ are defined as

$$\begin{aligned} A_i &= C_9^{\mathrm{eff}} \frac{f_i - g_i}{2} - \frac{2m_b}{q^2} C_7 \frac{f_i^T + g_i^T}{2}, \\ B_i &= C_9^{\mathrm{eff}} \frac{f_i + g_i}{2} - \frac{2m_b}{q^2} C_7 \frac{f_i^T - g_i^T}{2}, \\ D_j &= C_{10} \frac{f_j - g_j}{2}, \\ E_j &= C_{10} \frac{f_j + g_j}{2}. \end{aligned} \tag{5}$$

Using the transition amplitude (4), the double differential decay rate is given by

$$\frac{\mathrm{d}^2\Gamma}{\mathrm{d}\hat{s}\,\mathrm{d}z} = \frac{G_F^2\,\alpha^2}{2^{12}\pi^5} |V_{tb} V_{ts}^*|^2\, m_{\Lambda_b}\, v_l\, \lambda^{1/2}(1, r, \hat{s})\, \mathcal{K}(\hat{s}, z), \tag{6}$$

where

$$\mathcal{K}(\hat{s}, z) = \mathcal{K}_0(\hat{s}) + z\,\mathcal{K}_1(\hat{s}) + z^2\,\mathcal{K}_2(\hat{s}), \tag{7}$$

$\hat{s} = s/m_{\Lambda_b}^2$ and $z = \hat{p}_B \cdot \hat{p}_l^+$ is the angle between the momenta of Λ_b and l^+ in the dilepton invariant mass frame. The complete expressions for $\mathcal{K}_0(\hat{s})$, $\mathcal{K}_1(\hat{s})$ and $\mathcal{K}_2(\hat{s})$ are given in appendix B. Here $v_l = \sqrt{1 - (4m_l^2/q^2)}$ and $\lambda(1, r, \hat{s}) = (1 - r)^2 - 2\hat{s}(1 + r) + \hat{s}^2$ is the triangle function with $r = m_\Lambda/m_{\Lambda_b}$. The physical allowed range for $s \equiv q^2$ is

$$4m_l^2 \leqslant s \leqslant (m_{\Lambda_b} - m_\Lambda)^2. \tag{8}$$

Another interesting observable is the zero-crossing of the forward–backward asymmetry, wherein the position of the zero value of the forward–backward asymmetry parameter (A_{FB}) is very useful to look for the NP signal. The normalised forward–backward asymmetry is defined as

$$A_{\mathrm{FB}}(\hat{s}) = \frac{\int_0^1 \frac{\mathrm{d}^2\Gamma}{\mathrm{d}\hat{s}\,\mathrm{d}z}\mathrm{d}z - \int_{-1}^0 \frac{\mathrm{d}^2\Gamma}{\mathrm{d}\hat{s}\,\mathrm{d}z}\mathrm{d}z}{\int_0^1 \frac{\mathrm{d}^2\Gamma}{\mathrm{d}\hat{s}\,\mathrm{d}z}\mathrm{d}z + \int_{-1}^0 \frac{\mathrm{d}^2\Gamma}{\mathrm{d}\hat{s}\,\mathrm{d}z}\mathrm{d}z}, \tag{9}$$

which can be simplified to

$$A_{\mathrm{FB}}(\hat{s}) = \frac{\mathcal{K}_1(\hat{s})}{\mathcal{K}_0(\hat{s}) + \mathcal{K}_2(\hat{s})/3}. \tag{10}$$

The polarisation asymmetries P_i ($i = L, N, T$) are defined as

$$P_i(\hat{s}) = \frac{\frac{\mathrm{d}\Gamma}{\mathrm{d}\hat{s}}(\hat{\eta} = \hat{e}_i) - \frac{\mathrm{d}\Gamma}{\mathrm{d}\hat{s}}(\hat{\eta} = -\hat{e}_i)}{\frac{\mathrm{d}\Gamma}{\mathrm{d}\hat{s}}(\hat{\eta} = \hat{e}_i) + \frac{\mathrm{d}\Gamma}{\mathrm{d}\hat{s}}(\hat{\eta} = -\hat{e}_i)}, \tag{11}$$

where $\hat{e}_i$'s are the unit vectors along the longitudinal, normal and transverse components of the l^+ polarisation and $\hat{\eta}$ is a unit vector, used to write the l^+ four-spin vector (s_+), along the l^+ spin in its rest frame as

$$s_+^0 = \frac{\vec{p}_+ \cdot \hat{\eta}}{m_l}, \quad \vec{s}_+ = \hat{\eta} + \frac{s_+^0}{E_{l^+} + m_l}\vec{p}_+. \tag{12}$$

Thus, the observables P_L, P_T and P_N correspond to longitudinal, transverse and normal polarisation asymmetries respectively. The observables P_L and P_T are P-odd, T-even, while P_N is P-even, T-odd and CP-odd. The explicit expressions for forward–backward asymmetry and all the polarisation parameters are taken from [16, 18, 19].

Another interesting observable is the lepton universality violation (LUV) parameter, which has been recently observed by the LHCb collaboration in $B^+ \to K^+ l^+ l^-$ process and has 2.6σ deviation from its SM predicted value [6]. Analogously, we define the parameter (R_Λ) as the ratio of branching fractions of $\Lambda_b \to \Lambda l^+ l^-$ into dimuon over dielectron as

$$R_\Lambda = \frac{\mathrm{Br}(\Lambda_b \to \Lambda \mu^+ \mu^-)}{\mathrm{Br}(\Lambda_b \to \Lambda e^+ e^-)}. \tag{13}$$

3. NP contribution due to scalar leptoquark exchange

In this section we will consider the effect of scalar leptoquarks to the $\Lambda_b \to \Lambda l^+ l^-$ decay processes. The exchange of leptoquarks will contribute additional operators to the SM effective Hamiltonian and thus, the various observables may deviate significantly from their corresponding SM values. The scalar leptoquark multiplets with representations $X\,(3,\,2,\,7/6)$ and $X\,(3,\,2,\,1/6)$ under the SM gauge group $SU\,(3)_C \times SU\,(2)_L \times U\,(1)_Y$ conserve baryon and lepton numbers and do not allow proton decay. These baryon and lepton number conserving scalar leptoquarks can have sizable Yukawa couplings and could be light enough to be accessible in accelerator searches. Thus, they could potentially contribute to the $b \to s l^+ l^-$ transitions and one can constrain the underlying couplings from experimental data on $B_s \to l^+ l^-$ processes as well as from $B_s - \bar{B}_s$ mixing.

The interaction Lagrangian of the scalar leptoquarks $X = (3,\,2,\,7/6)$ with the SM bilinear fermions is given as [33, 34]

$$\mathcal{L} = -\lambda_u^{ij}\,\bar{u}_R^i X^T \epsilon L_L^j - \lambda_e^{ij}\,\bar{e}_R^i X^\dagger Q_L^j + \mathrm{h.c.}, \tag{14}$$

where $i,\,j$ are the generation indices, X is the leptoquark doublet, $Q_L\,(L_L)$ denotes the left handed quark (lepton) doublet, the right handed up-type quark (charged lepton) singlet is represented by $u_R\,(e_R)$ and $\epsilon = \mathrm{i}\sigma_2$ is a 2×2 matrix. The multiplets defined above are represented as

$$X = \begin{pmatrix} V_\alpha \\ Y_\alpha \end{pmatrix}, \quad Q_L = \begin{pmatrix} u_L \\ d_L \end{pmatrix}, \quad \text{and} \quad L_L = \begin{pmatrix} \nu_L \\ e_L \end{pmatrix}. \tag{15}$$

Now expanding the $SU(2)$ indices, the interaction Lagrangian (14) takes the form

$$\mathcal{L} = -\lambda_u^{ij}\,\bar{u}_{\alpha R}^i (V_\alpha e_L^j - Y_\alpha \nu_L^j) - \lambda_e^{ij}\,\bar{e}_R^i (V_\alpha^\dagger u_{\alpha L}^j + Y_\alpha^\dagger d_{\alpha L}^j) + \mathrm{h.c.}. \tag{16}$$

Thus, from equation (16) one can obtain the interaction Hamiltonian for $b \to s l_i^+ l_i^-$ processes after performing the Fierz transformation as

$$\mathcal{H}_{\mathrm{LQ}} = \frac{\lambda_e^{i3}\lambda_e^{i2*}}{8M_Y^2}[\bar{s}\gamma^\mu(1-\gamma_5)b][\bar{l}_i\gamma_\mu(1+\gamma_5)l_i] = \frac{\lambda_e^{i3}\lambda_e^{i2*}}{4M_Y^2}(O_9 + O_{10}). \tag{17}$$

Comparing (17) with the corresponding SM effective Hamiltonian (1), one can obtain the new Wilson coefficients as

$$C_9^{\mathrm{NP}} = C_{10}^{\mathrm{NP}} = -\frac{\pi}{2\sqrt{2}\,G_{\mathrm{F}}\alpha V_{tb}V_{ts}^*}\frac{\lambda_e^{i3}\lambda_e^{i2*}}{M_Y^2}. \tag{18}$$

Similarly, the interaction Lagrangian due to the exchange of the scalar leptoquark $X = (3,\,2,\,1/6)$ is

$$\mathcal{L} = -\lambda_d^{ij}\,\bar{d}_{\alpha R}^i (V_\alpha e_L^j - Y_\alpha \nu_L^j) + \mathrm{h.c.}, \tag{19}$$

which contributes to the primed Wilson coefficients ($C'_{9,10}$) corresponding to the semileptonic electroweak penguin operators $\mathcal{O}'_{9,10}$ (i.e., the right-handed counter parts of the SM operators $\mathcal{O}_{9,10}$) and are given as

$$C_9'^{\mathrm{NP}} = -C_{10}'^{\mathrm{NP}} = \frac{\pi}{2\sqrt{2}\;G_{\mathrm{F}}\alpha V_{tb}V_{ts}^*}\frac{\lambda_s^{2i}\lambda_b^{3i*}}{M_V^2}. \tag{20}$$

Thus, from the above equations (18) and (20), one can find that there are four additional Wilson coefficients $C_{9,10}^{(\prime)\mathrm{NP}}$, which will contribute to the $b \to s l^+ l^-$ processes due to the scalar leptoquark exchange. Thus, the modified parameters (5) in the amplitude (4), become

Table 1. Constraints on the leptoquark couplings obtained from various leptonic $B_s \to l^+l^-$ decays [29], where M_S denotes the mass of the scalar LQ.

Decay Process	Couplings involved	Bound on the LQ couplings (GeV^{-2})
$B_s \to \mu^\pm\mu^\mp$	$\frac{\lvert\lambda^{32}\lambda^{22*}\rvert}{M_S^2}$	$<5.0 \times 10^{-9}$
$B_s \to e^\pm e^\mp$	$\frac{\lvert\lambda^{31}\lambda^{21*}\rvert}{M_S^2}$	$<2.54 \times 10^{-5}$
$B_s \to \tau^\pm\tau^\mp$	$\frac{\lvert\lambda^{33}\lambda^{23*}\rvert}{M_S^2}$	$<1.2 \times 10^{-8}$

$$
\begin{aligned}
A_i &= C_9'^{\text{NP}}\frac{f_i+g_i}{2} + (C_9^{\text{eff}} + C_9^{\text{NP}})\frac{f_i-g_i}{2} - \frac{2m_b}{q^2}C_7^{\text{SM}}\frac{f_i^T+g_i^T}{2},\\
B_i &= (C_9^{\text{eff}} + C_9^{\text{NP}})\frac{f_i+g_i}{2} - \frac{2m_b}{q^2}C_7^{\text{SM}}\frac{f_i^T-g_i^T}{2} + C_9'^{\text{NP}}\frac{f_i-g_i}{2},\\
D_j &= C_{10}'^{\text{NP}}\frac{f_j+g_j}{2} + (C_{10}^{\text{SM}} + C_{10}^{\text{NP}})\frac{f_j-g_j}{2},\\
E_j &= (C_{10}^{\text{SM}} + C_{10}^{\text{NP}})\frac{f_j+g_j}{2} + C_{10}'^{\text{NP}}\frac{f_j-g_j}{2}.
\end{aligned}
\tag{21}
$$

Next, we have to find out the constraints on the leptoquark couplings to see how various observables behave in the LQ model. The detailed calculation of the constraint on the new leptoquark parameter space has been presented in [29–31], therefore here we will simply quote the main results. We constrain the leptoquark coupling by comparing the theoretical [44] and experimental [45–47] branching ratios of $B_s \to l^+l^-$ processes and the $B_s - \bar{B}_s$ mixing data [8]. For completeness, here we briefly outline the procedure for obtaining the constraints from $B_s \to \mu^+\mu^-$ process and $B_s - \bar{B}_s$ mixing, however, the technical details can be found in [29–31].

3.1. Constraint from $B_s \to \mu^+\mu^-$ process

In the leptoquark model the branching ratio for the $B_s \to \mu^+\mu^-$ mode can be given as

$$
\begin{aligned}
\text{Br}(B_s \to \mu^+\mu^-) &= \frac{G_F^2}{16\pi^3}\tau_{B_s}\alpha^2 f_{B_s}^2 M_{B_s} m_\mu^2 |V_{tb}V_{ts}^*|^2 |C_{10}^{\text{SM}} + C_{10}^{\text{NP}} - C_{10}'^{\text{NP}}|^2 \sqrt{1-\frac{4m_\mu^2}{M_{B_s}^2}}\\
&= \text{Br}^{\text{SM}} \left| 1 + \frac{C_{10}^{\text{NP}} - C_{10}'^{\text{NP}}}{C_{10}^{\text{SM}}} \right|^2 \equiv \text{Br}^{\text{SM}}\, |1 + re^{i\phi^{\text{NP}}}|^2,
\end{aligned}
\tag{22}
$$

where Br^{SM} is the SM branching ratio and the parameters r and ϕ^{NP} are defined as

$$
re^{i\phi^{\text{NP}}} = \frac{C_{10}^{\text{NP}} - C_{10}'^{\text{NP}}}{C_{10}^{\text{SM}}}. \tag{23}
$$

Now comparing the SM theoretical prediction of $\text{Br}(B_s \to \mu^+\mu^-)$ [44]

$$
\text{Br}(B_s \to \mu^+\mu^-)|_{\text{SM}} = (3.65 \pm 0.23) \times 10^{-9}, \tag{24}
$$

with the corresponding experimental value [45–47]

$$
\text{Br}(B_s \to \mu^+\mu^-) = (2.9 \pm 0.7) \times 10^{-9}, \tag{25}
$$

and assuming that each individual leptoquark contribution to the branching ratio does not exceed the experimental result, one can obtain the bound on the NP parameters r and ϕ^{NP}. The allowed parameter space in $r - \phi^{\text{NP}}$ plane which is compatible with the 1σ range of the experimental data is

$$
0 \leqslant r \leqslant 0.35, \quad \text{with} \quad \pi/2 \leqslant \phi^{\text{NP}} \leqslant 3\pi/2. \tag{26}
$$

These bounds can be translated to obtain the bounds for the leptoquark couplings as

$$
0 \leqslant \frac{|\lambda_\mu^{23}\lambda_\mu^{22*}|}{M_Y^2} = \frac{|\lambda_s^{22}\lambda_b^{32*}|}{M_V^2} \leqslant 5 \times 10^{-9}\ \text{GeV}^{-2} \quad \text{for} \quad \pi/2 \leqslant \phi^{\text{NP}} \leqslant 3\pi/2. \tag{27}
$$

Similarly, one can obtain the upper bound on the product of various combination of leptoquark couplings from $B_s \to l^+l^-$ processes which are presented in table 1. Using the bounds on leptoquark couplings one can obtain the constraints on new Wilson coefficients using the equations (18) and (20).

3.2. Constraint from $B_s - \bar{B}_s$ mixing

In this subsection, we will discuss the constraint on leptoquark couplings from the $B_s - \bar{B}_s$ mixing, which in the SM, proceeds through the box diagram with internal top quark and W boson exchange. The effective Hamiltonian describing the $\Delta B = 2$ transition is given as [48]

$$\mathcal{H}_{\rm eff} = \frac{G_F^2}{16\pi^2}\,|V_{tb}V_{ts}^*|^2\,M_W^2\,S_0(x_t)\,\eta_B\,(\bar{s}b)_{V-A}\,(\bar{s}b)_{V-A}, \tag{28}$$

where η_B is the QCD correction factor and $S_0(x_t)$ is the loop function given in [48].

Thus, the $B_s - \bar{B}_s$ mixing amplitude in the SM, can be written as

$$M_{12}^{\rm SM} = \frac{1}{2M_{B_s}}\langle \bar{B}_s|\mathcal{H}_{\rm eff}|B_s\rangle = \frac{G_F^2}{12\pi^2}M_W^2\,|V_{tb}V_{ts}^*|^2\,\eta_B\,\hat{B}_s f_{B_s}^2\,M_{B_s}\,S_0(x_t). \tag{29}$$

The corresponding mass difference can be computed from the mixing amplitude through $\Delta M_s = 2|M_{12}|$. Now using the particle masses from [8], $\eta_B = 0.551$, the Bag parameter $\hat{B}_{B_s} = 1.320 \pm 0.017 \pm 0.030$ and the decay constant $f_{B_s} = 225.6 \pm 1.1 \pm 5.4$ from [49], the value of ΔM_s in the SM, is found as

$$\Delta M_s^{\rm SM} = (17.426 \pm 1.057)\ {\rm ps}^{-1}, \tag{30}$$

which is in good agreement with the experimental result [8]

$$\Delta M_s = 17.761 \pm 0.022\ {\rm ps}^{-1}. \tag{31}$$

For $X(3,\ 2,\ 7/6)$ LQ, the mixing amplitude receives additional contribution from leptoquark and charged lepton in the box diagram whereas for $X(3,\ 2,\ 1/6)$ both charged lepton and neutrino will contribute to the mixing amplitude. The effective Hamiltonian due to the leptoquark $X(3,\ 2,\ 7/6)$ is given by

$$\mathcal{H}_{\rm eff} = \sum_{i=e,\mu,\tau}\frac{(\lambda^{bi}\lambda^{si*})^2}{128\pi^2}\frac{1}{M_S^2}\,I\left(\frac{m_i^2}{M_S^2}\right)(\bar{b}\gamma^\mu P_L s)(\bar{b}\gamma_\mu P_L s), \tag{32}$$

and for $X(3,\ 2,\ 1/6)$ leptoquark the corresponding effective Hamiltonian becomes

$$\mathcal{H}_{\rm eff} = \sum_{i=e,\mu,\tau}\frac{(\lambda^{bi*}\lambda^{si})^2}{128\pi^2}\left[\frac{1}{M_S^2}\,I\left(\frac{m_i^2}{M_S^2}\right)+\frac{1}{M_S^2}\right](\bar{b}\gamma^\mu P_R s)(\bar{b}\gamma_\mu P_R s). \tag{33}$$

where the loop function $I(x)$ is given as

$$I(x) = \frac{1 - x^2 + 2x\log x}{(1-x)^2}. \tag{34}$$

Thus, the contribution to the mixing amplitude due to the exchange of scalar leptoquark is given by

$$\begin{aligned} M_{12}^{\rm LQ} &= \frac{(\lambda^{32*}\lambda^{22})^2}{192\pi^2 M_S^2}\eta_B\hat{B}_{B_s}f_{B_s}^2 M_{B_s}, \qquad \text{for } X(3,\ 2,\ 1/6),\\ M_{12}^{\rm LQ} &= \frac{(\lambda^{32}\lambda^{22*})^2}{384\pi^2 M_S^2}\eta_B\hat{B}_{B_s}f_{B_s}^2 M_{B_s}, \qquad \text{for } X(3,\ 2,\ 7/6). \end{aligned} \tag{35}$$

Including both the SM and leptoquark contributions the total mass difference is given as

$$\Delta M_s = \Delta M_s^{\rm SM}\left|\left[1+\frac{c}{16G_F^2|V_{tb}V_{ts}^*|^2 m_W^2 S_0(x_t)}\left(\frac{(\lambda^{32}\lambda^{22*})^2}{M_S^2}\right)\right]\right|, \tag{36}$$

where the constant $c = 1$ for $X(3,\ 2,\ 1/6)$ and $1/2$ for $X(3,\ 2,\ 7/6)$. Now varying the mass difference $(\Delta M_s/\Delta M_s^{\rm SM})$ within its 1σ allowed range [8], the constraint on $|\lambda^{32}\lambda^{22}/M_S|$ is found to be [31]

$$\begin{aligned} 0 \leqslant \left|\frac{\lambda^{32}\lambda^{22}}{M_S}\right| &\leqslant 7.5\times 10^{-5}\ {\rm GeV}^{-1}, \qquad \text{for } X(3,\ 2,\ 7/6),\\ 0 \leqslant \left|\frac{\lambda^{32}\lambda^{22}}{M_S}\right| &\leqslant 5.0\times 10^{-5}\ {\rm GeV}^{-1}, \qquad \text{for } X(3,\ 2,\ 1/6). \end{aligned} \tag{37}$$

In order to relate this results with the bounds obtained $B_s \to \mu\mu$ process, we scale the couplings obtained from $B_s - \bar{B}_s$ mass difference for a benchmark leptoquark mass of 1 TeV and the bounds in equation (37) is translated as

Table 2. Numerical values of the form factor $f_1(0)$, $f_2(0)$ and the parameters involved in the double fit for $\Lambda_b \to \Lambda$ transition.

Parameter	LCSR (twist-3) [21]
$f_1(0)$	$0.14^{+0.02}_{-0.01}$
a	$2.91^{+0.1}_{-0.07}$
b	$2.26^{+0.13}_{-0.08}$
$f_2(0)$ $(10^{-2}\,\mathrm{GeV}^{-1})$	$-0.47^{+0.06}_{-0.06}$
a	$3.4^{+0.06}_{-0.05}$
b	$2.98^{+0.09}_{-0.08}$

$$\begin{aligned} 0 \;&\leqslant\; |\frac{\lambda^{32}\lambda^{22}}{M_S^2}| \leqslant 7.5 \times 10^{-8}\,\mathrm{GeV}^{-2}, \qquad \text{for } X(3,\,2,\,7/6),\\ 0 \;&\leqslant\; |\frac{\lambda^{32}\lambda^{22}}{M_S^2}| \leqslant 5.0 \times 10^{-8}\,\mathrm{GeV}^{-2}, \qquad \text{for } X(3,\,2,\,1/6), \end{aligned} \tag{38}$$

which are reasonably higher than those of obtained from $B_s \to \mu\mu$ process. Hence in our analysis, we will use the bounds (26) as discussed in the previous subsection.

4. Numerical analysis

After having the detailed knowledge about the SM observables and the bound on the new leptoquark couplings, we now proceed for numerical analysis. We have taken the particle masses and the life time of Λ_b baryon from [8]. The q^2 dependence of form factors derived in the light cone sum rule (LCSR) approach can be parameterised as

$$f_i(q^2) = \frac{f_i(0)}{1 - a(q^2/m^2_{\Lambda_b}) + b(q^2/m^2_{\Lambda_b})^2}, \tag{39}$$

where the values of the parameters $f_i(0)$, a and b and are listed in table 2 [21]. The other form factors are related to these two and the HQET form factors ($F_{1,2}$) through [21]

$$\begin{aligned} f_2^T = g_2^T = f_1 = g_1 = F_1 + \frac{m_\Lambda}{m_{\Lambda_b}}F_2,\\ f_2 = g_2 = f_3 = g_3 = \frac{F_2}{m_{\Lambda_b}},\\ f_1^T = g_1^T = \frac{F_2}{m_{\Lambda_b}}q^2. \end{aligned} \tag{40}$$

In the lattice QCD formalism, the $\Lambda_b \to \Lambda$ helicity form factors, i.e., $f_{+,\perp,0}$, $g_{+,\perp,0}$, $h_{+,\perp}$ and $\tilde{h}_{+,\perp}$ in the physical limit can have the simple form [23]

$$f(q^2) = \frac{1}{1 - q^2/(m^f_{\mathrm{pole}})^2}[a_0^f + a_1^f z(q^2) + a_2^f [z(q^2)]^2], \tag{41}$$

where the values and uncertainties of the parameters a_0^f, a_1^f and a_2^f from the higher-order fit are given in table 5 of [23]. These helicity form factors are related to the form factors $f_i^{(T)}$ and $g_i^{(T)}$ used in this work as follows:

$$\begin{aligned} f_+ &= f_1 - \frac{q^2}{m_{\Lambda_b}+m_\Lambda}f_2, \quad f_\perp = f_1 - (m_{\Lambda_b}+m_\Lambda)f_2, \quad f_0 = f_1 + \frac{q^2}{m_{\Lambda_b}-m_\Lambda}f_3,\\ g_+ &= g_1 + \frac{q^2}{m_{\Lambda_b}-m_\Lambda}g_2, \quad g_\perp = g_1 + (m_{\Lambda_b}-m_\Lambda)g_2, \quad g_0 = g_1 - \frac{q^2}{m_{\Lambda_b}+m_\Lambda}g_3,\\ h_+ &= f_2^T - \frac{m_{\Lambda_b}+m_\Lambda}{q^2}f_1^T, \quad h_\perp = f_2^T - \frac{f_1^T}{m_{\Lambda_b}+m_\Lambda},\\ \tilde{h}_+ &= g_2^T + \frac{m_{\Lambda_b}-m_\Lambda}{q^2}g_1^T, \quad \tilde{h}_\perp = g_2^T + \frac{g_1^T}{m_{\Lambda_b}-m_\Lambda}. \end{aligned} \tag{42}$$

In our analysis, we have taken the form factors computed in the LCSR approach for low q^2 region (as these are not so well-behaved in the high q^2 regime), and for high q^2 theory we have used the lattice QCD calculations of $\Lambda_b \to \Lambda$ form factors [23]. The values of the Wilson coefficients used in our analysis are evaluated at the

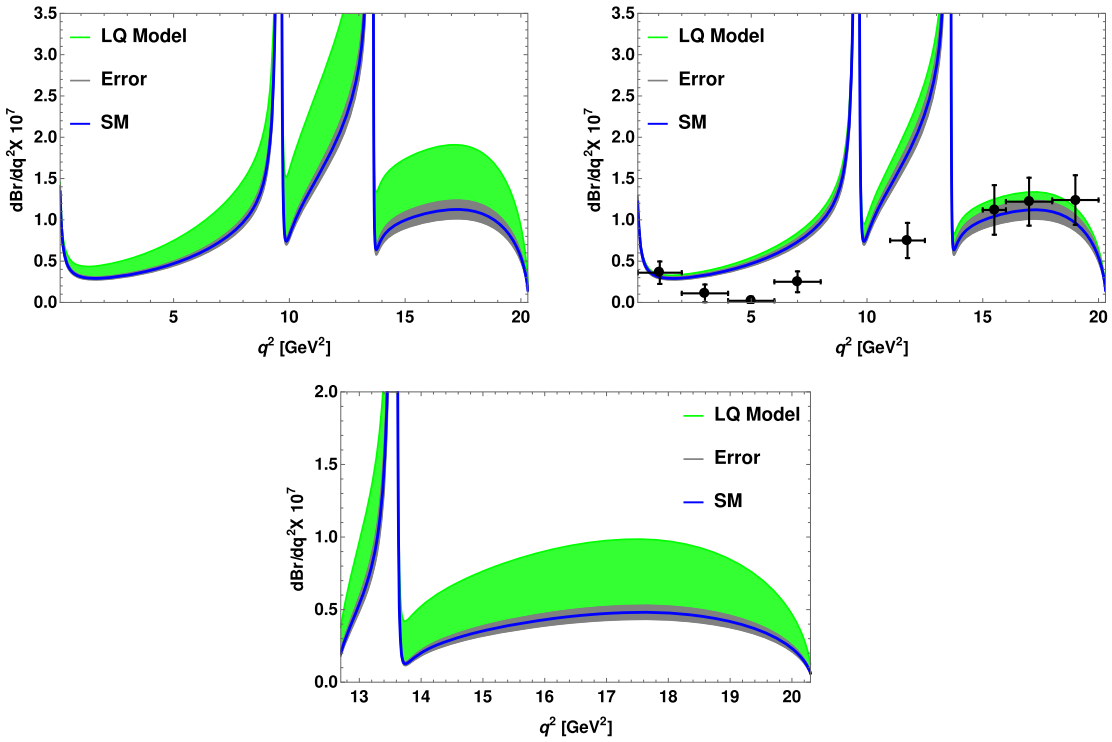

Figure 1. The variation of branching ratio of $\Lambda_b \to \Lambda e^+e^-$ (left panel), $\Lambda_b \to \Lambda\mu^+\mu^-$ (right panel) and $\Lambda_b \to \Lambda\tau^+\tau^-$ (bottom panel) with respect to low and high q^2 including the LD contributions, both in the SM and in the $X = (3,\ 2,\ 7/6)$ leptoquark model. In each plot, the green band represents the leptoquark contribution and the blue solid line is for the SM. The grey band represents the theoretical uncertainty arises due to the input parameters in the SM. The black data points in $\Lambda_b \to \Lambda\mu^+\mu^-$ process represent the bin-wise experimental data.

renormalisation scale $\mu \approx m_b = 4.8$ GeV. In the LQ model, the NP contributions to the branching ratios and forward–backward asymmetry parameters are encoded in the new Wilson coefficients. By using the above input parameters and the values of the new Wilson coefficients, we show in figure 1, the q^2 variation of branching ratio of $\Lambda_b \to \Lambda e^+e^-$ (top left panel), $\Lambda_b \to \Lambda\mu^+\mu^-$ (top right panel) and $\Lambda_b \to \Lambda\tau^+\tau^-$ (bottom panel) processes for the full kinematically accessible physical region. In these plots, we have shown the contributions arising from the exchange of $X = (3,\ 2,\ 7/6)$ leptoquark. The SM contributions are represented by blue lines and the grey bands denote the theoretical uncertainties arising due to the uncertainties associated with the CKM matrix elements and the hadronic form factors. The green bands represent the leptoquark contributions to the branching ratios. The bin-wise experimental results for $\Lambda_b \to \Lambda\mu^+\mu^-$ process [15] are shown by black data points. There is slight deviation in the decay distribution between the predicted and observed data. The corresponding results coming from the exchange of the $X = (3,\ 2,\ 1/6)$ LQ are shown in figure 2. From these figures, one can see that the branching ratios of $\Lambda_b \to \Lambda e^+e^-$ and $\Lambda_b \to \Lambda\tau^+\tau^-$ decay processes deviate significantly from their SM predictions, whereas the NP effects on $\Lambda_b \to \Lambda\mu^+\mu^-$ branching ratio is not so prominent. In table 3, we present the integrated values of branching ratio for all the above processes, where we have used the veto windows as ($8\ \text{GeV}^2 < m^2_{l^+l^-} < 11\ \text{GeV}^2$) and ($12.5\ \text{GeV}^2 < m^2_{l^+l^-} < 15\ \text{GeV}^2$) [15], to eliminate the backgrounds coming from the dominant resonances $\Lambda_b \to \Lambda J/\psi(\psi')$ with $J/\psi(\psi') \to l^+l^-$. The predicted branching ratio for $\Lambda_b \to \Lambda\mu^+\mu^-$ is almost consistent with the observed data $\text{Br}(\Lambda_b \to \Lambda\mu^+\mu^-) = (1.08 \pm 0.28) \times 10^{-6}$ [8]. Also, as seen from table 3, the experimental result can be accommodated in the leptoquark model. Within the SM, the forward backward asymmetry parameters in the $B \to Kl^+l^-$ decay processes are identically zero since they only involve scalar and tensor types of currents, whereas $B \to Kl^+l^-$ processes are described by only vector-type interactions. However, for semileptonic $\Lambda_b \to \Lambda l^+l^-$ decay processes, the forward backward asymmetry depends on two combinations of the Wilson coefficients $\text{Re}(C_7^{\text{eff}} C_{10}^*)$ and $\text{Re}(C_9^{\text{eff}} C_{10}^*)$ [16] and thus, can have negative values in the SM. The contribution due to the new Wilson coefficients ($C_{9,10}^{\text{NP}(\prime)}$) may enhance the rate of asymmetries and can shift the zero position of these asymmetries. In figure 3, the variation of forward–backward asymmetry for $\Lambda_b \to \Lambda\mu^+\mu^-$ (left panel), $\Lambda_b \to \Lambda\tau^+\tau^-$ (right panel) modes are depicted with respect to q^2 both in the SM and in the $X = (3,\ 2,\ 7/6)$ LQ model including the LD contributions and the corresponding integrated values are presented in table 3. Similarly the variation of forward–backward asymmetries for $X = (3,\ 2,\ 1/6)$ LQ exchange are shown in figure 4. We found no significant deviation of the zero position of A_{FB} from its SM value due to the leptoquark contributions in $\Lambda_b \to \Lambda\mu^+\mu^-$ process. However, there is certain discrepancy between the observed and predicted results in

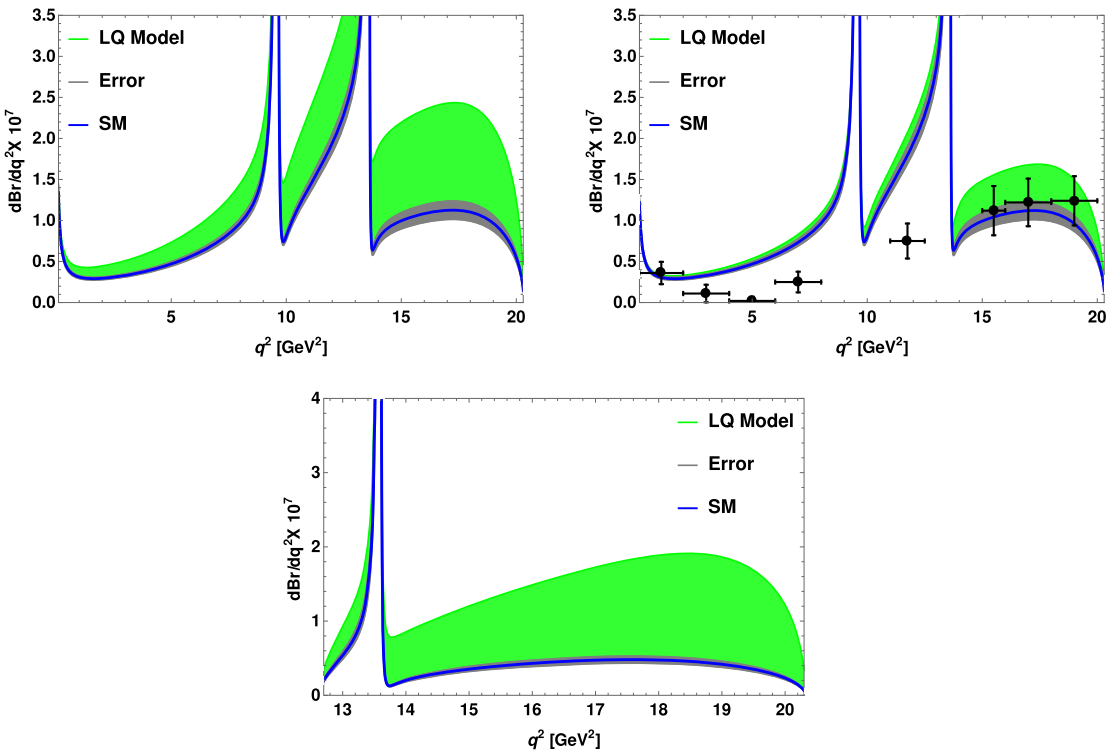

Figure 2. Same as figure 1 for $X = (3,\ 2,\ 1/6)$ LQ exchange.

Table 3. The predicted integrated values of the branching ratio, forward–backward asymmetry, lepton polarisation asymmetry and the lepton non-universality with respect to their respective q^2 range for the $\Lambda_b \to \Lambda\mu(\tau)^+\mu(\tau)^-$ processes in the SM and the LQ model.

Observables	SM prediction	Values in $Y = 7/6$ LQ model	Values in $Y = 1/6$ LQ model
$\mathrm{Br}(\Lambda_b \to \Lambda e^+e^-)$	$(1.168 \pm 0.134) \times 10^{-6}$	$(1.168 - 1.91) \times 10^{-6}$	$(1.168 - 2.13) \times 10^{-6}$
$\mathrm{Br}(\Lambda_b \to \Lambda\mu^+\mu^-)$	$(1.165 \pm 0.132) \times 10^{-6}$	$(1.165 - 1.37) \times 10^{-6}$	$(1.165 - 1.52) \times 10^{-6}$
$\langle A_{\mathrm{FB}}^{\mu}\rangle$	-0.567	$-0.567 \to -0.446$	$-0.567 \to -0.54$
$\langle P_L^{\mu}\rangle$	0.34	$0.3 - 0.34$	$0.24 - 0.34$
$\langle P_T^{\mu}\rangle$	-4.5×10^{-4}	$-(4.5 \to 2.87) \times 10^{-4}$	$-(0.45 \to 3.26) \times 10^{-3}$
$\langle P_N^{\mu}\rangle$	-0.0192	$-0.0192 \to -0.013$	$-0.0192 \to -0.012$
$\mathrm{Br}(\Lambda_b \to \Lambda\tau^+\tau^-)$	$(2.13 \pm 0.215) \times 10^{-7}$	$(2.13 - 4.38) \times 10^{-7}$	$(2.13 - 8.32) \times 10^{-7}$
$\langle A_{\mathrm{FB}}^{\tau}\rangle$	-0.38	$-0.38 \to 3.2 \times 10^{-3}$	$-0.38 \to 7.68 \times 10^{-2}$
$\langle P_L^{\tau}\rangle$	0.075	$0.047 - 0.075$	$6.3 \times 10^{-3} - 0.075$
$\langle P_T^{\tau}\rangle$	-2.3×10^{-3}	$-(7 \to 2.3) \times 10^{-3}$	$(-0.23 \to 2.0) \times 10^{-2}$
$\langle P_N^{\tau}\rangle$	-0.05	$-0.05 \to 8.1 \times 10^{-3}$	$-0.05 \to 0.0316$
$\langle R_{\Lambda_b}^{\mu e}\rangle$	0.997	$0.67 - 0.997$	$0.68 - 0.997$
$\langle R_{\Lambda_b}^{\mu e}\rangle_{[q^2\in(1,6)]}$	0.998	$0.71 - 0.998$	$0.74 - 0.998$

the high q^2 regime. The forward–backward asymmetry for $\Lambda_b \to \Lambda\tau^+\tau^-$ process however, has significant deviation from the SM in both the $X = (3,\ 2,\ 7/6)$ and $X = (3,\ 2,\ 1/6)$ leptoquark model. Besides the branching ratios and forward–backward asymmetry parameters of $\Lambda_b \to \Lambda l^+l^-$ processes, the NP effects can also be observed in the lepton polarisation asymmetries. In the left panel of figure 5, the distribution of the longitudinal (top), transverse (middle) and normal (bottom) polarisation components for $\Lambda_b \to \Lambda\mu^+\mu^-$ process are shown both in the SM and in the $X = (3,\ 2,\ 7/6)$ LQ model, and the corresponding plots for $\Lambda_b \to \Lambda\tau^+\tau^-$ process are presented in the right panel. The integrated values of all the three polarisations in the full physical phase space have been presented in table 3. In figure 6, we have shown the variation of the different polarisation parameters for $\Lambda_b \to \Lambda\mu^+\mu^-$ process in the $X = (3,\ 2,\ 1/6)$ leptoquark model. It is found from table 3, that the transverse and normal polarisation values are very small in the SM and even the leptoquark model does not give any significant deviation.

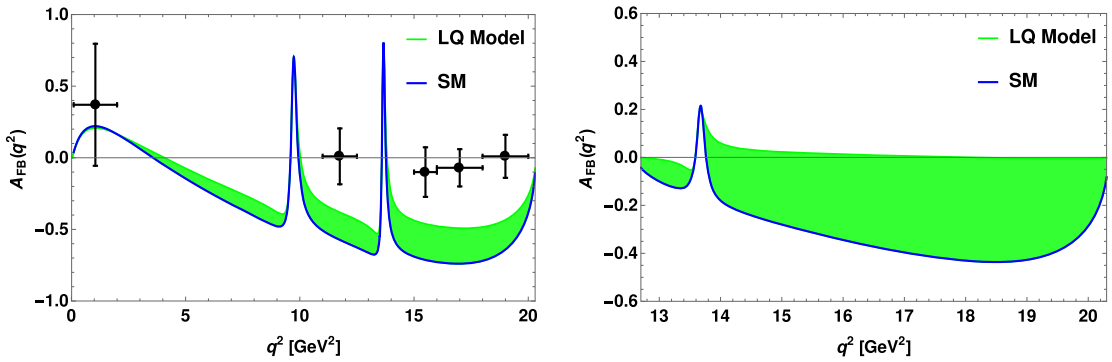

Figure 3. The forward–backward asymmetry variation of $\Lambda_b \to \Lambda\mu^+\mu^-$ (left panel) and $\Lambda_b \to \Lambda\tau^+\tau^-$ (right panel) with respect to q^2 for $X = (3,\ 2,\ 7/6)$ LQ exchange. The black data points in $\Lambda_b \to \Lambda\mu^+\mu^-$ process represent the bin-wise experimental data.

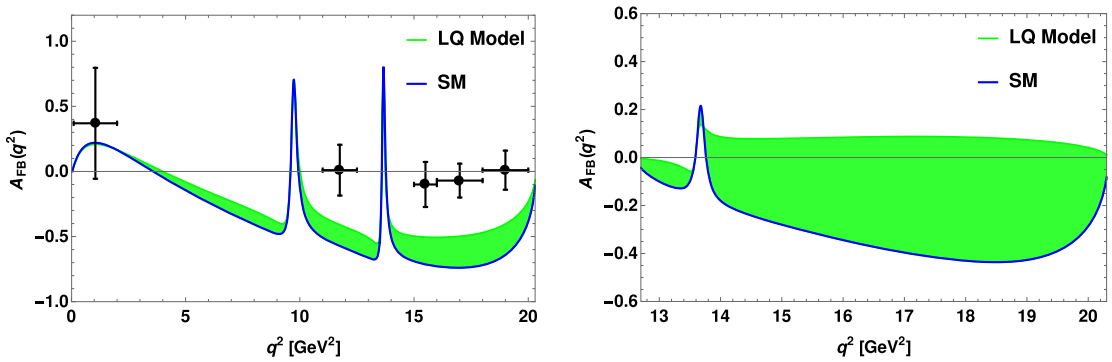

Figure 4. Same as figure 3 for $X = (3,\ 2,\ 1/6)$ LQ exchange.

Analogous to the lepton flavour non-universality parameter R_K, i.e., the ratio of branching fractions of $B \to K\mu^+\mu^-$ over $B \to Ke^+e^-$, we would like to see whether it is possible to observe lepton non-universality in the Λ_b decays. We have define these parameters as e.g., $R_\Lambda^{\mu e} = \mathrm{Br}(\Lambda_b \to \Lambda\mu^+\mu^-)/\mathrm{Br}(\Lambda_b \to \Lambda e^+e^-)$. In figure 7, we show the variation of lepton nonuniversality parameter $R_\Lambda^{\mu e}$ (top-right panel), $R_\Lambda^{\tau e}$ (bottom-left panel) and $R_\Lambda^{\tau\mu}$ (bottom-right panel) in their respective q^2 region. Also, we show the low-q^2 behaviour of $R_\Lambda^{\mu e}$ (top-left panel), in the range $1 \leqslant q^2 \leqslant 6$ GeV^2. These results are for $X = (3,\ 2,\ 7/6)$ leptoquark. Similarly the lepton nonuniversality plot for $X = (3,\ 2,\ 1/6)$ leptoquark exchange is shown in figure 8. The integrated values of the lepton non-universality parameter in both SM and LQ model are presented in table 3. We found that there is significant violation of lepton universality in Λ_b decays, though there is no experimental evidence so far. The violation of lepton universality is more pronounced for the processes having τ as final particle. However, as the reconstruction of tau events are extremely difficult, this observable may not be sensitive enough to be observed in near future. As seen from the top-left panel of figures 7 and 8, the parameter $R_\Lambda^{\mu e}$ is very promising for the Belle II experiment, as the LHCb, being a hadronic machine works better in muon mode than electron.

5. LFV $\Lambda_b \to \Lambda l_i^- l_j^+$ decays

In this section, we will compute the branching ratios of LFV Λ_b decays mediating through the exchange of scalar leptoquarks. The LFV decay processes are extremely rare in the SM as they are either two-loop suppressed with tiny neutrino masses in one of the loop or proceed through box diagram (which is also highly suppressed due to tiny neutrino mass). However, they can occur at tree level in the LQ model and are expected to have significantly large branching fractions. The observation of neutrino oscillation has provided unambiguous evidence for lepton flavour violation in the neutral lepton sector which in turn provides motivation to explore other LFV transitions such as $l_i \to l_j\gamma$, $l_i^- \to l_j^- l_k^+ l_k^-$, $B \to l_i^\pm l_j^\mp$ etc. Though there is no direct experimental evidence for such processes, but there exists experimental upper bounds on some of these modes. The LFV decays in the B meson and in the charged lepton sector have been widely investigated in the literature [29, 36, 50]. Therefore, it is interesting to see whether LFV decays could be observed in Λ_b decays also.

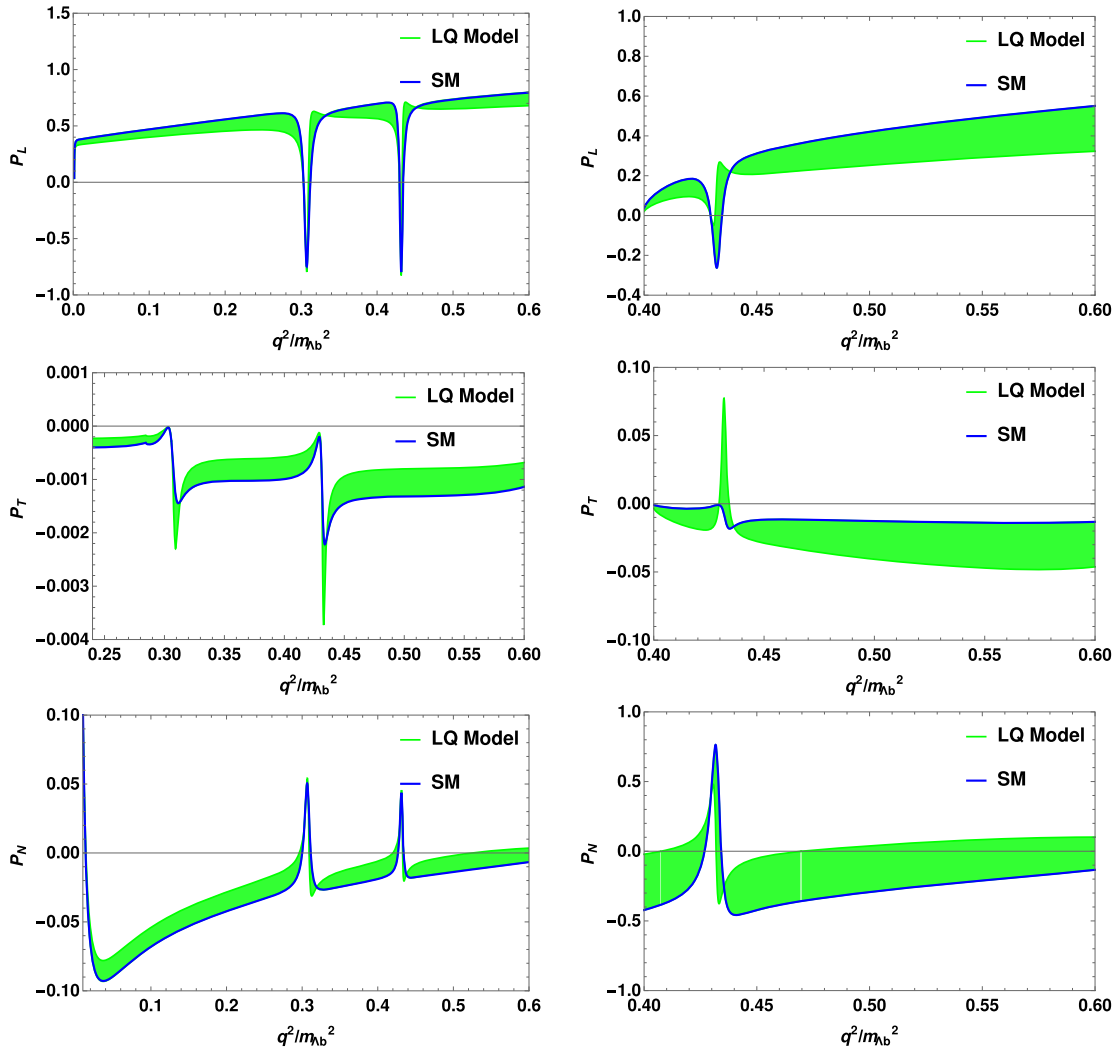

Figure 5. The plots in the left panel represent the longitudinal (top), transverse (middle) and normal (bottom) polarisations for $\Lambda_b \to \Lambda\mu^+\mu^-$ precess with respect to $q^2/m^2_{\Lambda_b}$ in the $X = (3,\ 2,\ 7/6)$ LQ model. The corresponding plots for $\Lambda_b \to \Lambda\tau^+\tau^-$ mode are shown in the right panel.

As discussed earlier, these processes occur at tree level due to the exchange of scalar leptoquarks. In the leptoquark model the effective Hamiltonian for $b \to s l_i^- l_j^+$ LFV process is given as [29, 36]

$$\mathcal{H}_{\rm LQ} = G_{\rm LQ}\,(\bar{s}\gamma^\mu P_L b)(\bar{l}_i\gamma_\mu(1+\gamma_5)l_j), \tag{43}$$

where the coefficient $G_{\rm LQ}$ is

$$G_{\rm LQ} = \frac{\lambda^{i3}\lambda^{j2*}}{8M_Y^2}. \tag{44}$$

Using the form factors given in the appendix A, the amplitude for the LFV $\Lambda_b \to \Lambda l_i^- l_j^+$ decay is given by

$$\begin{aligned}\mathcal{M}(\Lambda_b \to \Lambda l_i^- l_j^+) \;=\; & G_{\rm LQ}\,[(\bar{l}_i\gamma_\mu(1+\gamma_5)l_j)\{\bar{u}_\Lambda(\gamma^\mu(A_1' P_R + B_1' P_L))u_{\Lambda_b} \\ & + \bar{u}_\Lambda \mathrm{i}\sigma_{\mu\nu}q^\nu(A_2' P_R + B_2' P_L)u_{\Lambda_b} + q^\mu\bar{u}_\Lambda(A_3' P_R + B_3' P_L)u_{\Lambda_b}\}].\end{aligned} \tag{45}$$

The coefficients A_k' and B_k' in (45) are related to the form factors through

$$A_k' = \frac{f_k - g_k}{2} \quad \text{and} \quad B_k' = \frac{f_k + g_k}{2}, \quad k = 1,\ 2,\ 3. \tag{46}$$

Now using this transition amplitude, the branching ratio for the $\Lambda_b \to \Lambda l_i^- l_j^+$ process is given as

$$\frac{\mathrm{d}^2\Gamma}{\mathrm{d}\hat{s}\,\mathrm{d}\cos\theta} = \frac{|G_{\rm LQ}|^2}{2^6\pi^3} m_{\Lambda_b}^5 \frac{\sqrt{\lambda_1\lambda_2}}{\hat{s}} I(\hat{s}), \tag{47}$$

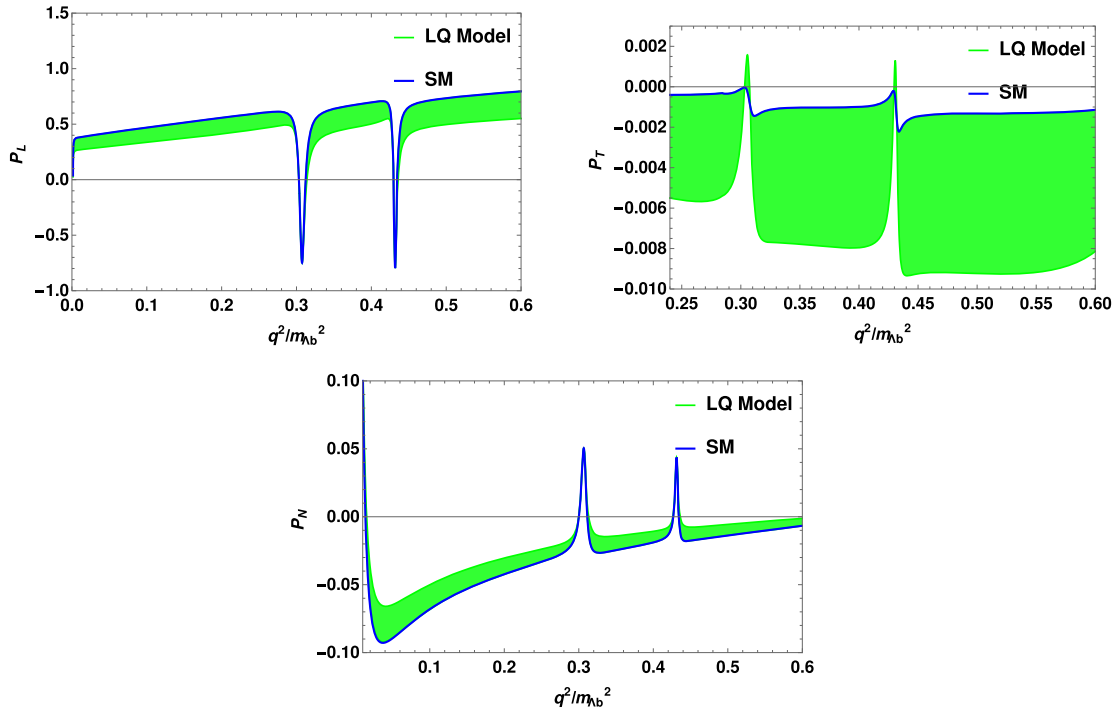

Figure 6. The polarisation plots of $\Lambda_b \to \Lambda\mu^+\mu^-$ process for $X = (3,\ 2,\ 1/6)$ LQ exchange.

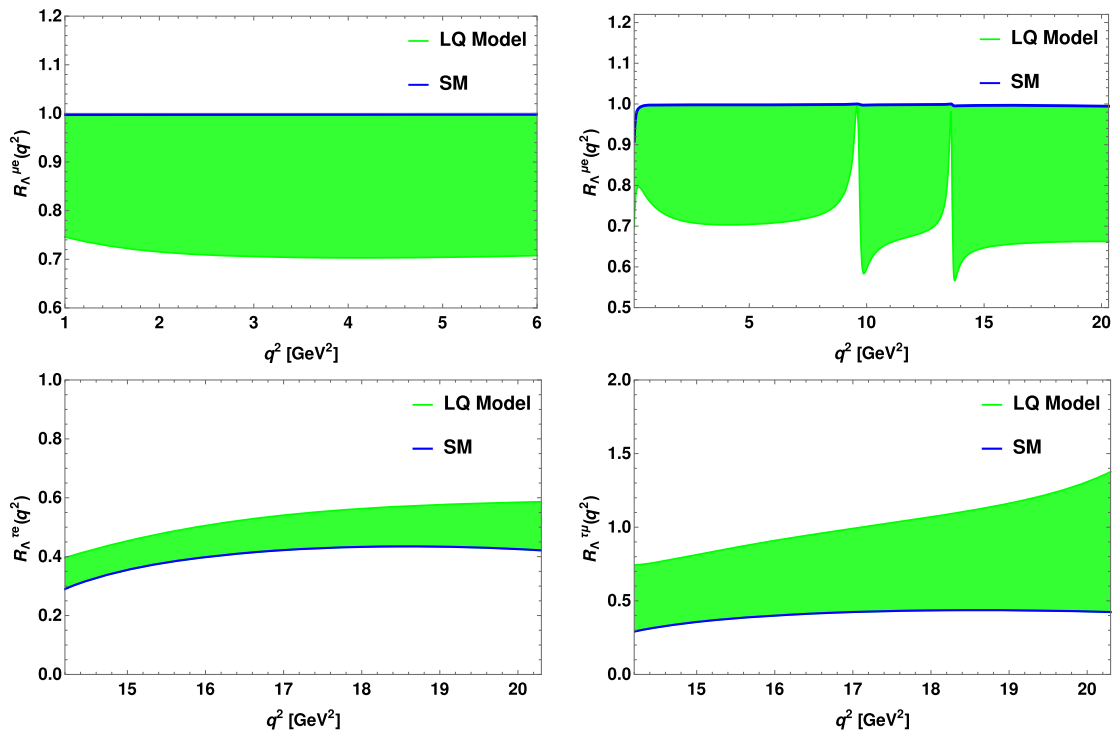

Figure 7. The variation of lepton universality violation $R_\Lambda^{\mu e}$ (top-right panel), $R_\Lambda^{\tau e}$ (bottom-left panel) and $R_\Lambda^{\tau\mu}$ (bottom-right panel) with respect to q^2 for $X = (3,\ 2,\ 7/6)$ LQ exchange. Here $R_\Lambda^{\mu e}$ (top-left panel) shows the non-universality in the low $q^2 \in [1,\ 6]$ region.

where

$$I(\hat{s}) = I_0(\hat{s}) + I_1(\hat{s})\cos\theta + I_2(\hat{s})\cos^2\theta, \tag{48}$$

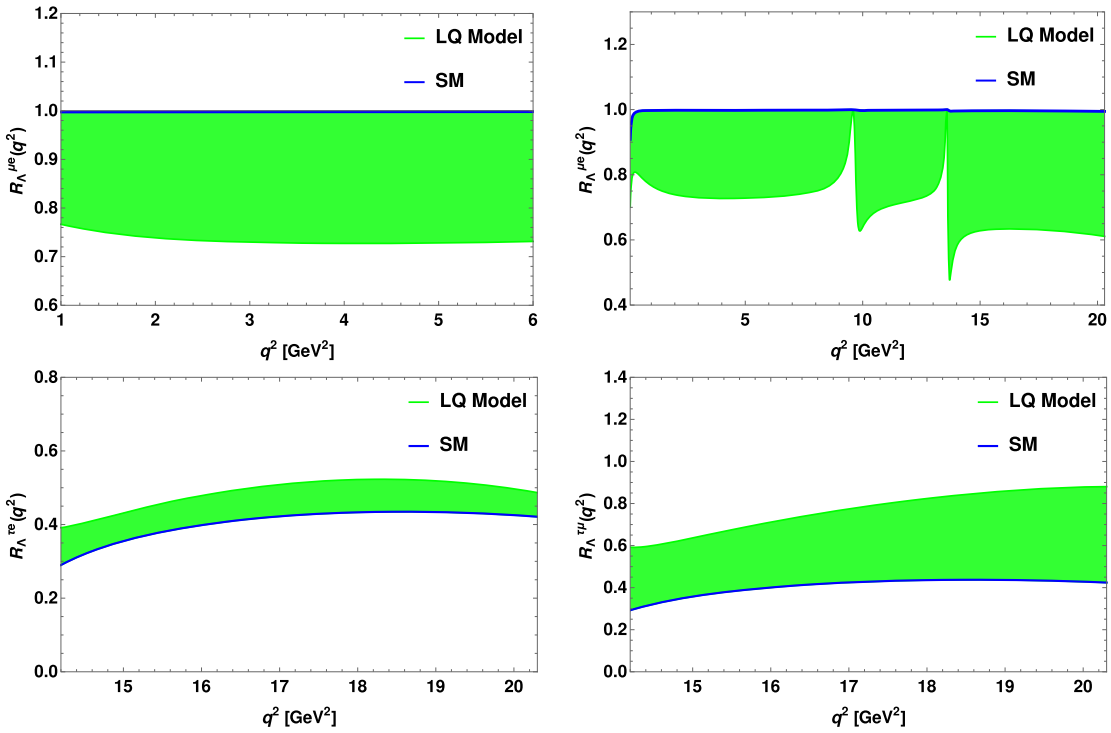

Figure 8. Same as figure 7 for $X = (3,\ 2,\ 1/6)$ LQ exchange.

with

$$
\begin{aligned}
I_0(\hat{s}) = \frac{1}{4}&(|A_1'|^2 + |B_1'|^2 + m_{\Lambda_b}^2\hat{s}\,(|A_2'|^2 + |B_2'|^2))[(1-r)^2 - \hat{s}^2] \\
&- 2\sqrt{r}\hat{s}\left(1 - \frac{m_i^2 + m_j^2}{q^2}\right)(\mathrm{Re}(A_1'B_1'^*) + m_{\Lambda_b}^2\hat{s}\mathrm{Re}(A_2'B_2'^*)) \\
&- \mathrm{Re}(A_2'B_2'^*)\sqrt{r}\left[-\frac{(m_i^2 - m_j^2)^2}{m_{\Lambda b}^2} + \hat{s}\,(m_i^2 + m_j^2)\right] \\
&+ 2m_{\Lambda_b}\hat{s}\left(1 - \frac{(m_i^2 + m_j^2)}{2q^2}\right)[(\mathrm{Re}(A_1'A_2'^*) + \mathrm{Re}(B_1'B_2'^*))\sqrt{r}\,(1-t) \\
&- (\mathrm{Re}(A_1'B_2'^*) + \mathrm{Re}(B_1'A_2'^*))(t-r)] \\
&+ \frac{(m_i^2 + m_j^2)}{m_{\Lambda_b}}[(\mathrm{Re}(A_1'A_3'^*) + \mathrm{Re}(B_1'B_3'^*))\sqrt{r}\,(1-t) + (\mathrm{Re}(A_1'B_3'^*) + \mathrm{Re}(B_1'A_3'^*))(t-r)] \\
&+ \left[\hat{s}\,(m_i^2 + m_j^2) - \frac{(m_i^2 - m_j^2)^2}{m_{\Lambda_b}^2}\right]\left[\frac{t}{2}(|A_3'|^2 + |B_3'|^2) - \sqrt{r}\mathrm{Re}(A_3'B_3'^*)\right],
\end{aligned}
\tag{49}
$$

$$
\begin{aligned}
I_1(\hat{s}) = \frac{\sqrt{\lambda_1\lambda_2}}{\hat{s}}&\left[-\frac{1}{2}\hat{s}\,(|A_1'|^2 - |B_1'|^2) + (m_j^2 - m_i^2)(1 - t - \frac{\hat{s}}{2})(|A_2'|^2 + |B_2'|^2)\right. \\
&+ \frac{1}{2}\frac{m_j^2 - m_i^2}{m_{\Lambda_b}}[\sqrt{r}\,(\mathrm{Re}(A_1'A_2'^*) + \mathrm{Re}(B_1'B_2'^*)) - (\mathrm{Re}(A_1'B_2'^*) + \mathrm{Re}(B_1'A_2'^*))] \\
&+ \frac{1}{2}\frac{m_j^2 - m_i^2}{m_{\Lambda_b}}[\sqrt{r}\,(\mathrm{Re}(A_1'A_3'^*) + \mathrm{Re}(B_1'B_3'^*)) + (\mathrm{Re}(A_1'B_3'^*) + \mathrm{Re}(B_1'A_3'^*))] \\
&\left.+ \frac{\hat{s}}{2}(m_i^2 - m_j^2)(\mathrm{Re}(A_2'A_3'^*) + \mathrm{Re}(B_2'B_3'^*))\right],
\end{aligned}
\tag{50}
$$

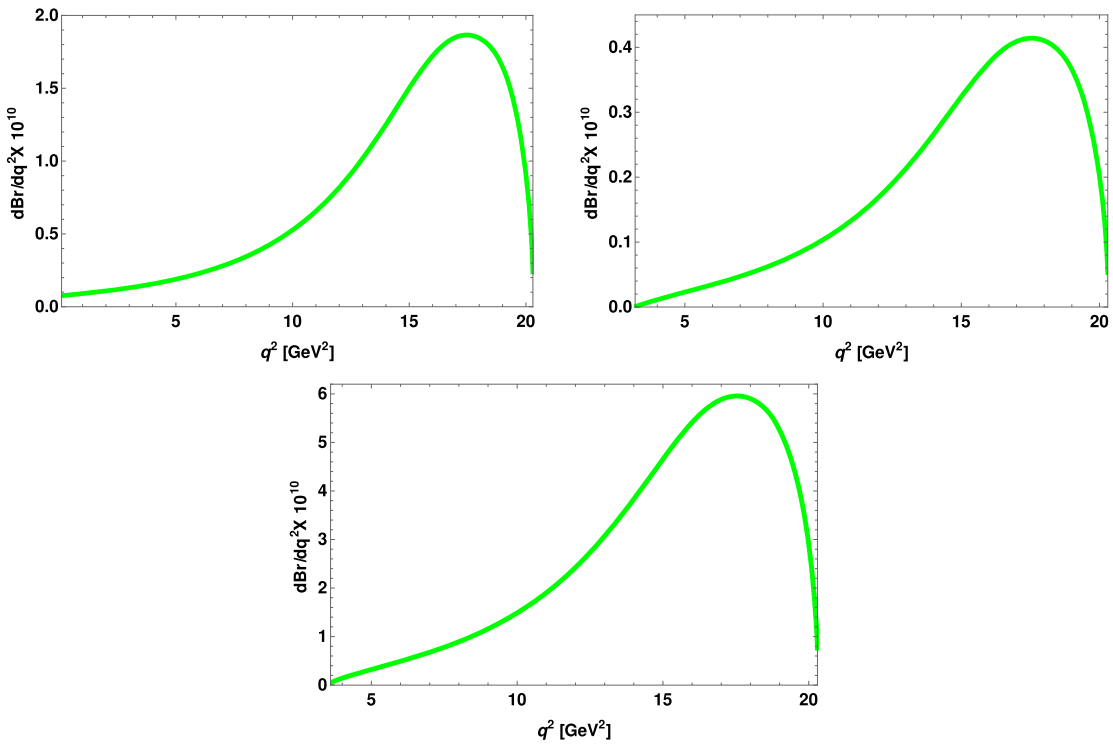

Figure 9. The variation of branching ratio of LFV $\Lambda_b \to \Lambda\mu^- e^+$ (left panel), $\Lambda_b \to \Lambda\tau^- e^+$ (right panel) and $\Lambda_b \to \Lambda\tau^-\mu^+$ (bottom panel) processes with respect to q^2 in the $X = (3,\ 2,\ 7/6)$ leptoquark model. Here the required leptoquark couplings are computed by using the scaling ansatz $\lambda^{ij} = (m_i/m_j)^{1/4}\lambda^{ii}$.

and

$$I_2(\hat{s}) = \frac{\lambda_1\lambda_2}{\hat{s}^2}\left[-\frac{1}{4}(|A_1'|^2 + |B_1'|^2 - m_{\Lambda_b}^2\hat{s}\,(|A_2'|^2 + |B_2'|^2))\right]. \tag{51}$$

Here, $\lambda_1 = \lambda$ (as defined in section 3), $\lambda_2 = \hat{m}_i^4 + \hat{m}_j^4 + \hat{s}^2 - 2(\hat{m}_i^2\hat{m}_j^2 + \hat{m}_i^2\hat{s} + \hat{m}_j^2\hat{s})$, and $t = (1 + r - \hat{s})/2$. The full kinematically accessible physical range for these processes is given by

$$(m_i + m_j)^2 \leqslant q^2 \leqslant (m_{\Lambda_b} - m_\Lambda)^2. \tag{52}$$

As there is no intermediate particle in the SM which can decay into two leptons of different flavours, so in comparison with the $\Lambda_b \to \Lambda l^+ l^-$ processes, LFV decays have no long distance QCD contributions and dominant charmonium resonance background. The required input values for numerical evaluation are taken from [8] and the values of the q^2 dependent form factors are taken from LCSR approach [21]. To determine the values of various LQ couplings, which are involved in the LFV decays, we use the following assumptions. As we know that the expansion parameter of the CKM matrix in the Wolfenstein parametrization (λ), can be related to the down type quark masses as $\lambda \sim (m_d/m_s)^{1/2}$ in the quark sector, while in the lepton sector one can have the same order for λ with the relation $\lambda \sim (m_{l_i}/m_{l_j})^{1/4}$. Hence, for other required leptoquark coupling, we assume that the coupling between different generation of quarks and leptons follow the simple scaling laws, i.e., $\lambda^{ij} = (m_i/m_j)^{1/4}\lambda^{ii}$ with $j > i$. Thus, using the values of the leptoquark coupling as given in table 1, one can obtain the bound on required LQ couplings involved in LFV decays. Using these values we plot the variation of branching ratio of LFV decays such as $\Lambda_b \to \Lambda\mu^- e^+$ (top left panel), $\Lambda_b \to \Lambda\tau^- e^+$ (top right panel) and $\Lambda_b \to \Lambda\tau^-\mu^+$ (lower panel) with respect to q^2 in figure 9 and the predicted upper limits of the branching ratios are given in table 4. So far there is no experimental evidence on the LFV Λ_b decays. However, since the predicted branching ratios are $\mathcal{O}(10^{-9})$, they can be searched at LHCb and exploration/observation of these modes would definitely shed some light in the leptoquark scenarios.

6. Conclusion

In this paper, we have studied the rare semileptonic $\Lambda_b \to \Lambda l^+ l^-$, $l = e,\ \mu,\ \tau$ baryonic decays in the scalar leptoquark model. The leptoquark parameter space has been constrained using the experimental limits on the branching ratios of the two body leptonic decays $B_s \to l^+ l^-$. We have computed the branching ratios, the forward–backward and lepton polarisation asymmetries ($P_{L,T,N}$) using the new leptoquark couplings. We have

Table 4. The predicted upper limits of the branching ratios, which are obtained using the upper limits of the LQ couplings, of LFV $\Lambda_b \to \Lambda l_i^- l_j^+$ processes, $l = e,\ \mu,\ \tau$ in the $X = (3,\ 2,\ 7/6)$ leptoquark model. Also the required leptoquark couplings are computed by using the scaling ansatz $\lambda^{ij} = (m_i/m_j)^{1/4}\lambda^{ii}$.

Decay process	Predicted branching ratio
$\Lambda_b \to \Lambda\mu^- e^+$	1.56×10^{-9}
$\Lambda_b \to \Lambda\tau^- e^+$	3.2×10^{-10}
$\Lambda_b \to \Lambda\tau^- \mu^+$	4.6×10^{-9}

shown explicitly the results for both the relevant $X = (3,\ 2,\ 7/6)$ and $X = (3,\ 2,\ 1/6)$ leptoquark models. The zero-position of the forward–backward asymmetry is found to be insensitive to the additional leptoquark effect. These models also give negligible contribution to the transverse polarisation asymmetry. In addition, we also estimated the LUV parameters in these decays analogous to R_K in $B \to Kl^+l^-$ process. The LFV Λ_b decays are also studied and the predicted upper limits on these branching ratios are found to be $\mathcal{O}(10^{-10} - 10^{-9})$, which could be searched in the LHCb experiment.

Acknowledgments

We would like to thank Science and Engineering Research Board (SERB) for financial support through grant No. SB/S2/HEP-017/2013.

Appendix A. Form factors in $\Lambda_b \to \Lambda$ transition

The transition form factors for $\Lambda_b(P) \to \Lambda(p')$ decays can be parameterised as [16, 43]

$$\begin{aligned}
\langle\Lambda(p')|\bar{s}\gamma_\mu b|\Lambda_b(P)\rangle &= f_1\bar{u}_\Lambda\gamma_\mu u_{\Lambda_b} + f_2\bar{u}_\Lambda i\sigma_{\mu\nu}q^\nu u_{\Lambda_b} + f_3 q_\mu \bar{u}_\Lambda u_{\Lambda_b},\\
\langle\Lambda(p')|\bar{s}\gamma_\mu\gamma_5 b|\Lambda_b(P)\rangle &= g_1\bar{u}_\Lambda\gamma_\mu\gamma_5 u_{\Lambda_b} + g_2\bar{u}_\Lambda i\sigma_{\mu\nu}q^\nu\gamma_5 u_{\Lambda_b} + g_3 q_\mu \bar{u}_\Lambda\gamma_5 u_{\Lambda_b},\\
\langle\Lambda(p')|\bar{s}i\sigma_{\mu\nu} b|\Lambda_b(P)\rangle &= f_T\bar{u}_\Lambda i\sigma_{\mu\nu}u_{\Lambda_b} + f_T^V\bar{u}_\Lambda(\gamma_\mu q_\nu - \gamma_\nu q_\mu)u_{\Lambda_b} + f_T^S(P_\mu q_\nu - P_\nu q_\mu)\bar{u}_\Lambda u_{\Lambda_b},\\
\langle\Lambda(p')|\bar{s}i\sigma_{\mu\nu}\gamma_5 b|\Lambda_b(P)\rangle &= g_T\bar{u}_\Lambda i\sigma_{\mu\nu}\gamma_5 u_{\Lambda_b} + g_T^V\bar{u}_\Lambda(\gamma_\mu q_\nu - \gamma_\nu q_\mu)\gamma_5 u_{\Lambda_b}\\
&\quad + g_T^S(P_\mu q_\nu - P_\nu q_\mu)\bar{u}_\Lambda\gamma_5 u_{\Lambda_b},
\end{aligned} \tag{A.1}$$

and for dipole operators

$$\langle\Lambda(p')|\bar{s}i\sigma_{\mu\nu}q^\nu b|\Lambda_b(P)\rangle = f_1^T\bar{u}_\Lambda\gamma_\mu u_{\Lambda_b} + f_2^T\bar{u}_\Lambda i\sigma_{\mu\nu}q^\nu u_{\Lambda_b} + f_3^T q_\mu\bar{u}_\Lambda u_{\Lambda_b}, \tag{A.2}$$

$$\langle\Lambda(p')|\bar{s}i\sigma_{\mu\nu}q^\nu\gamma_5 b|\Lambda_b(P)\rangle = g_1^T\bar{u}_\Lambda\gamma_\mu\gamma_5 u_{\Lambda_b} + g_2^T\bar{u}_\Lambda i\sigma_{\mu\nu}q^\nu\gamma_5 u_{\Lambda_b} + g_3^T q_\mu\bar{u}_\Lambda\gamma_5 u_{\Lambda_b}. \tag{A.3}$$

with $q = P - p'$ and

$$\begin{aligned}
f_2^T &= f_T - f_T^S q^2,\\
f_1^T &= [f_T^V + f_T^S(m_\Lambda + m_{\Lambda_b})]q^2,\\
f_1^T &= -\frac{q^2}{(m_{\Lambda_b} - m_\Lambda)}f_3^T,\\
g_2^T &= g_T - g_T^S q^2,\\
g_1^T &= [g_T^V + g_T^S(m_\Lambda - m_{\Lambda_b})]q^2,\\
g_1^T &= \frac{q^2}{(m_{\Lambda_b} + m_\Lambda)}g_3^T.
\end{aligned} \tag{A.4}$$

Appendix B. Expressions for $\mathcal{K}_{0,1,2}(\hat{s})$ functions

The complete expressions for $\mathcal{K}_{0,1,2}(\hat{s})$ functions required to calculate the double differential decay rate is given by [18]

$$\begin{aligned}\mathcal{K}_0(\hat{s}) = {} & 32m_l^2 m_{\Lambda_b}^2 \hat{s}(1+r-\hat{s})(|D_3|^2+|E_3|^2)\\ & + 64m_l^2 m_{\Lambda_b}^3(1-r-\hat{s})\mathrm{Re}(D_1^* E_3 + D_3 E_1^*) + 64m_{\Lambda_b}^2\sqrt{r}(6m_l^2 - \hat{s}m_{\Lambda_b}^2)\mathrm{Re}(D_1^* E_1)\\ & + 64m_l^2 m_{\Lambda_b}^3\sqrt{r}(2m_{\Lambda_b}\hat{s}\mathrm{Re}(D_3^* E_3) + (1-r+\hat{s})\mathrm{Re}(D_1^* D_3 + E_1^* E_3))\\ & + 32m_{\Lambda_b}^2(2m_l^2 + m_{\Lambda_b}^2\hat{s})((1-r+\hat{s})m_{\Lambda_b}\sqrt{r}\mathrm{Re}(A_1^* A_2 + B_1^* B_2)\\ & - m_{\Lambda_b}(1-r-\hat{s})\mathrm{Re}(A_1^* B_2 + A_2^* B_1) - 2\sqrt{r}[\mathrm{Re}(A_1^* B_1) + m_{\Lambda_b}^2\hat{s}\mathrm{Re}(A_2^* B_2)])\\ & + 8m_{\Lambda_b}^2(4m_l^2(1+r-\hat{s}) + m_{\Lambda_b}^2[(1-r)^2 - \hat{s}^2])(|A_1|^2+|B_1|^2)\\ & + 8m_{\Lambda_b}^4(4m_l^2[\lambda + (1+r-\hat{s})\hat{s}] + m_{\Lambda_b}^2\hat{s}[(1-r)^2 - \hat{s}^2])(|A_2|^2+|B_2|^2)\\ & - 8m_{\Lambda_b}^2(4m_l^2(1+r-\hat{s}) - m_{\Lambda_b}^2[(1-r)^2 - \hat{s}^2])(|D_1|^2+|E_1|^2)\\ & + 8m_{\Lambda_b}^5\hat{s}v_l^2(-8m_{\Lambda_b}\hat{s}\sqrt{r}\mathrm{Re}(D_2^* E_2) + 4(1-r+\hat{s})\sqrt{r}\mathrm{Re}(D_1^* D_2 + E_1^* E_2)\\ & - 4(1-r-\hat{s})\mathrm{Re}(D_1^* E_2 + D_2^* E_1) + m_{\Lambda_b}[(1-r)^2 - \hat{s}^2][|D_2|^2+|E_2|^2]), \end{aligned} \tag{B.1}$$

$$\begin{aligned}\mathcal{K}_1(\hat{s}) = {} & -16m_{\Lambda_b}^4\hat{s}v_l\sqrt{\lambda}\{2\mathrm{Re}(A_1^* D_1) - 2\mathrm{Re}(B_1^* E_1)\\ & + 2m_{\Lambda_b}\mathrm{Re}(B_1^* D_2 - B_2^* D_1 + A_2^* E_1 - A_1^* E_2)\}\\ & + 32m_{\Lambda_b}^5\hat{s}\, v_l\sqrt{\lambda}\{m_{\Lambda_b}(1-r)\mathrm{Re}(A_2^* D_2 - B_2^* E_2)\\ & + \sqrt{r}\mathrm{Re}(A_2^* D_1 + A_1^* D_2 - B_2^* E_1 - B_1^* E_2)\}, \end{aligned} \tag{B.2}$$

and

$$\begin{aligned}\mathcal{K}_2(\hat{s}) = {} & 8m_{\Lambda_b}^6 v_l^2\,\lambda\hat{s}\,((|A_2|^2+|B_2|^2+|D_2|^2+|E_2|^2)\\ & - 8m_{\Lambda_b}^4 v_l^2\,\lambda\,(|A_1|^2+|B_1|^2+|D_1|^2+|E_1|^2). \end{aligned} \tag{B.3}$$

References

[1] Aaij R *et al* (LHCb Collaboration) 2013 *Phys. Rev. Lett.* **111** 191801
[2] Aaij R *et al* (LHCb Collaboration) 2016 *J. High Energy Phys.* JHEP02(2016)104
[3] Abdesselam A *et al* (Belle Collaboration) arXiv:1604.04042
[4] Aaij R *et al* (LHCb Collaboration) 2014 *Phys. Rev. Lett.* **113** 151601
[5] Aaij R *et al* (LHCb Collaboration) 2014 *J. High Energy Phys.* JHEP06(2014)133
[6] Aaij R *et al* (LHCb Collaboration) 2013 *Phys. Rev. Lett.* **111** 191801
[7] Aaij R *et al* (LHCb Collaboration) 2013 *J. High Energy Phys.* JHEP07(2013)084
[8] Olive K A *et al* (Particle Data Group) 2014 *Chin. Phys.* C **38** 090001
[9] Descotes-Genon S, Matias J, Ramon M and Virto J 2013 *J. High Energy Phys.* JHEP01(2013)048
[10] Jager S and Camalich J M 2013 *J. High Energy Phys.* JHEP05(2013)043
Descotes-Genon S, Hofer L, Matias J and Virto J 2014 *J. High Energy Phys.* JHEP12(2014)125
[11] Descotes-Genon S, Hofer L, Matias J and Virto J 2016 *J. High Energy Phys.* JHEP06(2016)092
[12] Huber T, Hurth T and Lunghi E 2008 *Nucl. Phys.* B **802** 40
[13] Beaujean F, Bobeth C and van Dyk D 2014 *Eur. Phys. J.* C **74** 2897
Hurth T and Mahmoudi F 2014 *J. High Energy Phys.* JHEP04(2014)097
Altmannshofer W, Gori S, Pospelov M and Yavin I 2014 *Phys. Rev.* D **89** 095033
Hiller G and Schmaltz M 2014 *Phys. Rev.* D **90** 054014
Aristizabal Sierra D, Staub F and Vicente A 2015 *Phys. Rev.* D **92** 015001
Boucenna S M, Valle J W F and Vicente A 2015 *Phys. Lett.* B **750** 367–71
Mahmoudi F, Neshatpour S and Virto J 2014 *Eur. Phys. J.* C **74** 2927
Crivellin A, D'Ambrasio G and Heeck J 2015 *Phys. Rev. Lett.* **114** 151801
Crivellin A, D'Ambrasio G and Heeck J 2015 *Phys. Rev.* D **91** 075006
Crivellin A, Hofer L, Matias J, Nierste U, Pokorski S and Rosiek J 2015 *Phys. Rev.* D **92** 054013
Becirevic D, Fajfer S and Kosnik N 2015 *Phys. Rev.* D **92** 014016
Alonso R, Grinstein B and Camalich J M 2014 *Phys. Rev. Lett.* **113** 241802
Gripaios B, Nardecchia M and Renner S A 2015 *J. High Energy Phys.* JHEP05(2015)006
Falkowski A, Nardecchia M and Ziegler R 2015 *J. High Energy Phys.* JHE11(2015)173
Calibbi L, Crivellin A and Ota T 2015 *Phys. Rev. Lett.* **115** 181801
Descotes-Genon S, Matias J and Virto J 2013 *Phys. Rev.* D **88** 074002
[14] Meinel S and van Dyk D 2016 *Phys. Rev.* D **94** 013007
[15] Aaij R *et al* (LHCb Collaboration) 2015 *J. High Energy Phys.* JHEP06(2015)115
[16] Chen C-H and Geng C Q 2001 *Phys. Rev.* D **63** 054005
Chen C-H and Geng C Q 2001 *Phys. Rev.* D **63** 114024
Chen C-H and Geng C Q 2001 *Phys. Rev.* D **64** 074001
[17] Bashity V and Azizi K 2007 *J. High Energy Phys.* JHEP07(2007)064
[18] Giri A K and Mohanta R 2006 *Eur. Phys. J.* C **45** 151–8
Giri A K and Mohanta R 2005 *J. Phys.* G **31** 1559
Mohanta R and Giri A K 2010 *Phys. Rev.* D **82** 094022

[19] Chen C-H and Geng C Q 2001 *Phys. Lett.* B **516** 327
Huang C S and Han H J 1999 *Phys. Rev.* D **59** 114022
Huang C S and Han H J 2000 *Phys. Rev.* D **61** 039901 (erratum)
[20] Detmold W and Meinel S 2016 *Phys. Rev.* D **93** 074501
Kumar G and Mahajan N 2015 arXiv:1511.00935
Detmold W, David Lin C-J, Meinel S and Wingate M 2013 *Phys. Rev.* D **87** 074502
Azizi K and Katirci N 2012 *Eur. Phys. J.* A **48** 73
Aliev T M, Ozpineci A and Savci M 2003 *Nucl. Phys.* B **649** 168–88
Aliev T M, Ozpineci A and Savci M 2002 *Phys. Rev.* D **65** 115002
Aliev T M, Ozpineci A and Savci M 2003 *Phys. Rev.* D **67** 035007
Aliev T M, Ozpineci A and Savci M 2005 *Nucl. Phys.* B **709** 115
Aliev T M, Ozpineci A, Savci M and Yüce C 2002 *Phys. Lett.* B **542** 249
Gutsche T, Ivanov M A, Korner J G, Lyubovitskij V E and Santorelli P 2013 *Phys. Rev.* D **87** 074031
Boer P, Feldmann T and van Dyk D 2015 *J. High Energy Phys.* JHEP01(2015)155
Feldmann T and Yip M W Y 2012 *Phys. Rev.* D **85** 014035
Feldmann T and Yip M W Y 2012 *Phys. Rev.* D **86** 079901 (erratum)
[21] Wang Y-M, Li Y and Lu C-D 2009 *Eur. Phys. J.* C **59** 861
[22] Detmold W, David Lin C J, Meinel S and Wingate M 2013 *Phys. Rev.* D **87** 074502
[23] Detmold W and Meinel S 2016 *Phys. Rev.* D **93** 074501
[24] Georgi H and Glashow S L 1974 *Phys. Rev. Lett.* **32** 438
[25] Georgi H 1975 *AIP Conf. Proc.* **23** 575
Fritzsch H and Minkowski P 1975 *Ann. Phys.* **93** 193
Langacker P 1981 *Phys. Rep.* **72** 185
[26] Pati J C and Salam A 1974 *Phys. Rev.* D **10** 275
[27] Schrempp B and Shrempp F 1985 *Phys. Lett.* B **153** 101
Gripaios B 2010 *J. High Energy Phys.* JHEP02(2010)045
[28] Kaplan D B 1991 *Nucl. Phys.* B **365** 259
[29] Sahoo S and Mohanta R 2015 *Phys. Rev.* D **91** 094019
[30] Mohanta R 2014 *Phys. Rev.* D **89** 014020
[31] Sahoo S and Mohanta R 2016 *Phys. Rev.* D **93** 034018
[32] Davidson S, Bailey D C and Campbell B A 1994 *Z. Phys.* C **61** 613
Dorsner I, Fajfer S, Kamenik J F and Kosnik N 2009 *Phys. Lett.* B **682** 67
Fajfer S and Kosnik N 2009 *Phys. Rev.* D **79** 017502
Benbrik R, Chabab M and Faisel G 2010 arXiv:1009.3886
Povarov A V and Smirnov A D 2010 arXiv:1010.5707
Saha J P, Misra B and Kundu A 2010 *Phys. Rev.* D **81** 095011
Dorsner I, Drobnak J, Fajfer S, Kamenik J F and Kosnik N 2011 *J. High Energy Phys.* JHEP11(2011)002
Queiroz F S, Sinha K and Strumia A 2015 *Phys. Rev.* D **91** 035006
Allanach B, Alves A, Queiroz F S, Sinha K and Strumia A 2015 *Phys. Rev.* D **92** 055023
Ivo de M Varzielas and Hiller G 2005 *J. High Energy Phys.* JHEP06(2005)072
Sahoo S and Mohanta R 2016 *New J. Phys.* **18** 013032
Bauer M and Neubert M 2016 *Phys. Rev. Lett.* **116** 141802
Fajfer S and Kosnik N 2016 *Phys. Lett.* B **755** 270–4
[33] Arnold J M, Fornal B and Wise M B 2013 *Phys. Rev.* D **88** 035009
[34] Kosnik N 2012 *Phys. Rev.* D **86** 055004
[35] Aristizabal Sierra D, Hirsch M and Kovalenko S G 2008 *Phys. Rev.* D **77** 055011
Babu K S and Julio J 2010 *Nucl. Phys.* B **841** 130
Davidson S and Descotes-Genon S 2010 *J. High Energy Phys.* JHEP11(2010)073
Fajfer S, Kamenik J F, Nisandzic I and Zupan J 2012 *Phys. Rev. Lett.* **109** 161801
Cheung K, Keung W-Y and Tseng P-Y 2016 *Phys. Rev.* D **93** 015010
Camargo D A 2015 arXiv:1509.04263
Baek S and Nishiwaki K 2016 *Phys. Rev.* D **93** 015002
Pas H and Schumacher E 2015 *Phys. Rev.* D **92** 114025
Boucenna S M, Celis A, Fuentes-Martin J, Vicente A and Virto J 2016 *Phys. Lett.* B **760** 214
[36] Sahoo S and Mohanta R 2016 *Phys. Rev.* D **93** 114001
[37] Wang S-W and Yang Y-D 2016 arXiv:1608.03662
[38] Buchalla G, Buras A J and Lautenbacher M 1996 *Rev. Mod. Phys.* **68** 1125
[39] Altmannshofer W, Ball P, Bharucha A, Buras A J, Straub D M and Wick M 2009 *J. High Energy Phys.* JHEP01(2009)019
[40] Buras A J and Munz M 1995 *Phys. Rev.* D **52** 186
Misiak M 1993 *Nucl. Phys.* B **393** 23
Misiak M 1995 *Nucl. Phys.* B **439** 461 (erratum)
[41] Lim C S, Morozumi T and Sanda A I 1989 *Phys. Lett.* B **218** 343
Deshpande N G, Trampetic J and Ponose K 1989 *Phys. Rev.* D **39** 1461
O'Donnell P J and Tung H K K 1991 *Phys. Rev.* D **43** 2067
O'Donnell P J, Sutherland M and Tung H K K 1992 *Phys. Rev.* D **46** 4091
Krüger F and Sehgal L M 1996 *Phys. Lett.* B **380** 199
[42] Ali A, Ball P, Handoko L T and Hiller G 2000 *Phys. Rev.* D **61** 074024
[43] Mannel T, Roberts W and Ryzak Z 1991 *Nucl. Phys.* B **355** 38
Mannel T and Recksiegel S 1998 *J. Phys.* G **24** 979
[44] Bobeth C, Gorbahn M, Hermann T, Misiak M, Stamou E and Steinhauser M 2014 *Phys. Rev. Lett.* **112** 101801
[45] Chatrchyan S *et al* (CMS Collaboration) 2013 *Phys. Rev. Lett.* **111** 101805
[46] Aaij R *et al* (LHCb Collaboration) 2013 *Phys. Rev. Lett.* **111** 101805
[47] Khachatryan V *et al* (CMS Collaboration) and Bediaga I *et al* (LHCb Collaboration) 2015 *Nature* **522** 68

[48] Inami T and Lim C S 1981 *Prog. Theor. Phys.* **65** 297
Inami T and Lim C S 1981 *Prog. Theor. Phys.* **65** 1772 (erratum)
[49] Charles J *et al* 2015 *Phys. Rev.* D **91** 073007
[50] Ilakovac I and Pilaftsis A 1995 *Nucl. Phys.* B **437** 491
Barbieri R, Hall L H and Strumia A 1995 *Nucl. Phys.* B **445** 219
Hisano J, Moroi T, Tobe K and Yamaguchi M 1996 *Phys. Rev.* D **53** 2442
Ellis J R, Hisano J, Raidal M and Shimizu Y 2002 *Phys. Rev.* D **66** 115013
Brignole A and Rossi A 2004 *Nucl. Phys.* B **701** 3
Masiero A, Profumo S, Vempati S and Yaguna C E 2004 *J. High Energy Phys.* JHEP03(2004)046
Arganda A and Herrero M J 2006 *Phys. Rev.* D **73** 055003
Antusch A, Erganda E, Herrero M J and Teixeira A M 2006 *J. High Energy Phys.* JHEP11(2006)090
Paradisi P 2005 *J. High Energy Phys.* JHEP10(2005)006
Paradisi P 2006 *J. High Energy Phys.* JHEP02(2006)050
Paradisi P 2006 *J. High Energy Phys.* JHEP08(2006)047
Akeroyd A G, Aoki M and Okada Y 2007 *Phys. Rev.* D **76** 013004
Dassinger B M, Feldmann T, Mannel T and Turczyk S 2007 *J. High Energy Phys.* JHEP10(2007)039
Mohanta R 2011 *J. Euro Phys.* C **71** 1625
Alonso R, Grinstein B and Camalich J M 2015 arXiv:1505.05164
Lee C-J and Tandean J 2015 *J. High Energy Phys.* JHEP08(2015)123
Altmannshofer W and Yavin I 2015 *Phys. Rev.* D **92** 075022